

# Isostructural salts of the same complex showing contrasting thermal spin-crossover mediated by multiple phase changes†‡

Cite this: *Chem. Commun.*, 2013, **49**, 6280

Received 14th May 2013,  
Accepted 29th May 2013

DOI: 10.1039/c3cc43613f

www.rsc.org/chemcomm

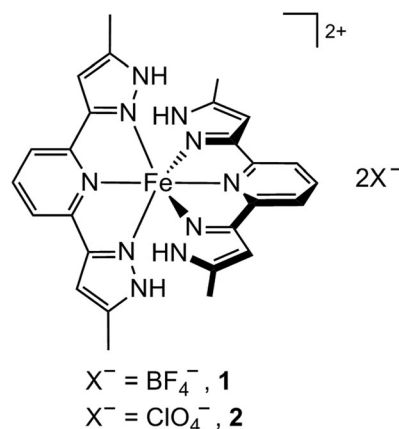
Thomas D. Roberts,<sup>a</sup> Marc A. Little,<sup>§a</sup> Floriana Tuna,<sup>b</sup> Colin A. Kilner<sup>a</sup> and Malcolm A. Halcrow<sup>\*a</sup>

**Two salts of  $[\text{FeL}_2]^{2+}$  (L = 2,6-bis[5-methyl-1H-pyrazol-3-yl]pyridine) are isostructural under ambient conditions but show different thermal spin-crossover behaviour, involving a variety of crystallographic phase changes.**

While an increasing number of applications for spin-crossover complexes<sup>1–6</sup> in devices and nanoscience has been demonstrated,<sup>3</sup> the number of materials showing technologically favourable spin-state switching is still very small.<sup>5</sup> There is therefore continued interest in the structural chemistry of spin-transition materials, which ultimately aims to crystal engineer new spin-crossover compounds with pre-defined functionality.<sup>6</sup>

We recently reported that  $[\text{FeL}_2][\text{BF}_4]_2$  (**1**; L = 2,6-bis(5-methyl-1H-pyrazol-3-yl)pyridine) adopts different anhydrous forms under slow crystallisation, and upon thermal dehydration of hydrated crystals.<sup>7</sup> The latter material undergoes an abrupt spin-transition around 205 K with wide thermal hysteresis, which is coupled to a sequence of three crystallographic phase changes (see below).<sup>7</sup> This behaviour, which was mostly elucidated by X-ray powder diffraction, makes **1** one of the most structurally complex spin-transition compounds known.<sup>6</sup> We now describe the corresponding perchlorate salt  $[\text{FeL}_2][\text{ClO}_4]_2$  (**2**), which is isostructural with **1** under ambient conditions, but exhibits very different spin-state properties.

As we have previously described, **1** usually crystallises from organic solvents as the brown hydrate  $1 \cdot 2\text{H}_2\text{O}$ , which contains two unique iron centres.<sup>7</sup> One of these is high-spin, and donates N–H...F hydrogen bonds to four  $\text{BF}_4^-$  anions. The other is low-spin,



and forms N–H...O interactions to four water molecules. An anhydrous phase of the same compound (phase **1<sup>A</sup>**) can also be obtained, which is structurally similar to  $1 \cdot 2\text{H}_2\text{O}$  but with the  $\text{BF}_4^-$  ions disordered onto the vacant water sites in the lattice. Exposure of **1<sup>A</sup>** to air leads to its rapid hydration to  $1 \cdot 2\text{H}_2\text{O}$ .

Heating  $1 \cdot 2\text{H}_2\text{O}$  to 400 K converts it to a different high-spin anhydrous material, **1<sup>B</sup>**, which is distinct from **1<sup>A</sup>** by powder diffraction. Cooling **1<sup>B</sup>** *in vacuo* leads to two consecutive phase changes **1<sup>B</sup>** → **1<sup>C</sup>** → **1<sup>D</sup>** near 303 and 270 K respectively, without changing its high-spin state. Phase **1<sup>D</sup>** then undergoes a cooperative transition to a fifth, low-spin phase **1<sup>E</sup>**. This spin-transition is centred near 205 K with a hysteresis loop of 37–65 K, depending on the history of the sample.

Unlike **1**, the structural chemistry of **2** is complicated by pseudopolymorphism. Recrystallisation of **2** from organic solvents often leads to mixtures of unsolvated and solvate phases. However, orange-yellow crystals of unsolvated **2** (phase **2<sup>A</sup>**) can be obtained in pure form by diffusion of diethyl ether into dilute methanol solutions of the complex at room temperature (more concentrated solutions instead afford the methanol solvate described below, which can be distinguished from **2<sup>A</sup>** by its brown colouration). Crystalline **2<sup>A</sup>** is isostructural with anhydrous phase **1<sup>A</sup>** although in contrast to **1<sup>A</sup>**, which is low-spin at 150 K, **2<sup>A</sup>** contains a residual high-spin fraction at that temperature by X-ray diffraction (ESI†). As for **1<sup>A</sup>**, crystals of **2<sup>A</sup>**

<sup>a</sup> School of Chemistry, University of Leeds, Woodhouse Lane, Leeds, UK LS2 9JT.

E-mail: m.a.halcrow@leeds.ac.uk; Fax: +44 (0)113 343 6565;

Tel: +44 (0)113 343 6506

<sup>b</sup> School of Chemistry and Photon Science Institute, University of Manchester, Oxford Road, Manchester, UK M13 9PL

† Celebrating 300 years of Chemistry at Edinburgh.

‡ Electronic Supplementary Information (ESI) available: Experimental descriptions, crystallographic figures and tables, and additional powder diffraction data. CCDC 936803–936805. For ESI and crystallographic data in CIF or other electronic format see DOI: 10.1039/c3cc43613f

§ Current address: Department of Chemistry, University of Liverpool, Crown Street, Liverpool, UK L69 7ZD.

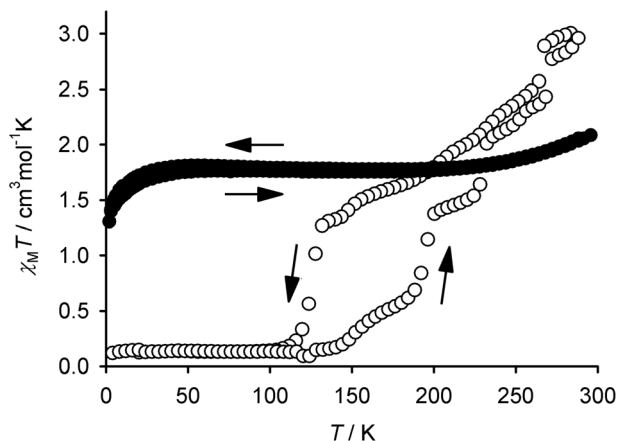


**Fig. 1** Comparison of the magnetic susceptibility behaviour of  $1\cdot 2\text{H}_2\text{O}$  (●)<sup>7</sup> and  $2\cdot 2\text{H}_2\text{O}$  (○) below room temperature. Both samples were scanned in both cooling and warming mode.

are hygroscopic and form brown  $2\cdot 2\text{H}_2\text{O}$  over a period of days on exposure to air at room temperature. The resultant crystals afford a similar unit cell to  $1\cdot 2\text{H}_2\text{O}$  at room temperature.<sup>¶7</sup> Moreover, bulk samples of  $1\cdot 2\text{H}_2\text{O}$  and  $2\cdot 2\text{H}_2\text{O}$  are isostructural at room temperature by X-ray powder diffraction (ESI†).

Despite their isostructural nature, the spin-state behaviour of  $1\cdot 2\text{H}_2\text{O}$  and  $2\cdot 2\text{H}_2\text{O}$  is very different (Fig. 1). Solid  $1\cdot 2\text{H}_2\text{O}$  exhibits an almost invariant 1:1 high:low-spin state population between 5–300 K.<sup>7</sup> In contrast, freshly prepared  $2\cdot 2\text{H}_2\text{O}$  is *ca.* 85% high-spin at room temperature, according to its  $\chi_{\text{M}}T$  value of  $3.1\text{ cm}^3\text{ mol}^{-1}\text{ K}$ . This value decreases on cooling, with a small discontinuity around 265 K (Fig. 1). More cooling leads  $\chi_{\text{M}}T$  to decrease further in a gradual but irregular manner until 120 K, when the remaining 25% of the sample undergoes a more abrupt spin-conversion, reaching its fully low-spin state at 110 K. Rewarming the sample shows the transition to exhibit a structured hysteresis below 200 K. The hysteresis loop spans 65 K at its widest point, and involves *ca.* 40% of the iron centres in the material. Repeated thermal cycling between 300–5–300 K caused some changes to the shape of the  $\chi_{\text{M}}T$  vs.  $T$  curve, although the discontinuity at 265 K and the low-temperature hysteresis were retained.

Variable temperature X-ray powder diffraction on  $2\cdot 2\text{H}_2\text{O}$  shed some light on these observations (Fig. 2). The discontinuity in  $\chi_{\text{M}}T$  at 265 K (Fig. 1) is associated with a crystallographic transformation to a new phase, labelled  $2\cdot 2\text{H}_2\text{O}^*$  in Fig. 2. This phase change is not exhibited by  $1\cdot 2\text{H}_2\text{O}$ .<sup>7</sup> The sample retains the  $2\cdot 2\text{H}_2\text{O}^*$  structure on cooling between 250–130 K, with only minor changes to the powder pattern being observed (Fig. 2). It is unclear whether the more abrupt part of the transition, that gives rise to the bulk of the hysteresis, involves a further crystallographic phase change at around 110 K.<sup>¶6–8</sup>

Heating  $2\cdot 2\text{H}_2\text{O}$  resulted in the loss of 1.5 equiv. of water at 368 K by thermogravimetric analysis (the highest temperature measured on safety grounds). Annealing  $2\cdot 2\text{H}_2\text{O}$  at 370 K leads to its conversion to a new yellow anhydrous phase  $2^{\text{B}}$ , which is isostructural with  $1^{\text{B}}$  and reverts to brown  $2\cdot 2\text{H}_2\text{O}$  on recooling in air. This transformation occurred rapidly in the powder diffractometer, where the sample was directly open to the vacuum (Fig. 2), but was more gradual in the magnetometer (ESI†).

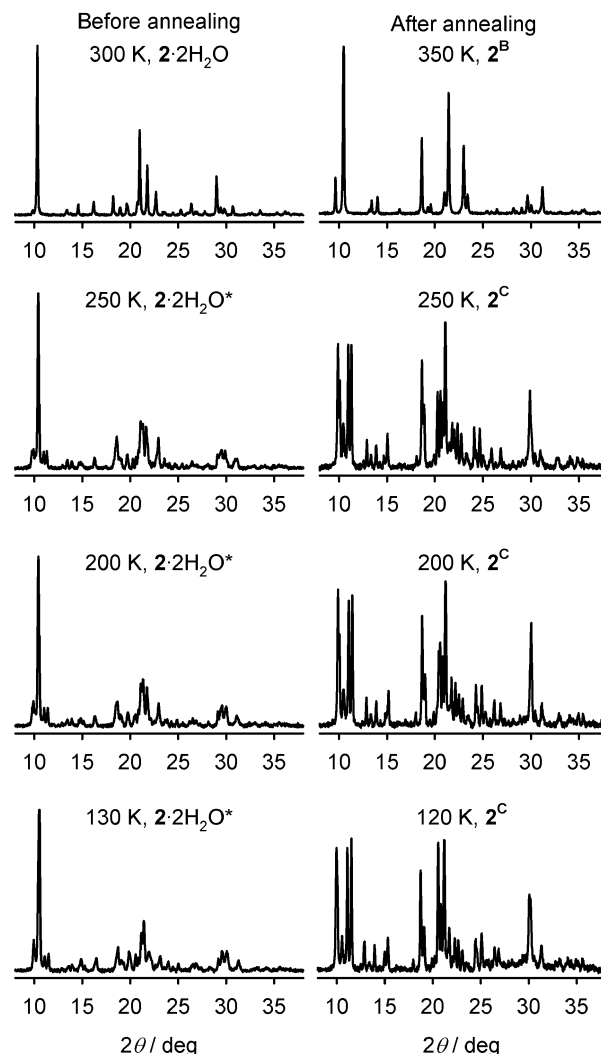


**Fig. 2** Variable temperature X-ray powder patterns of  $2\cdot 2\text{H}_2\text{O}$  before and after annealing at 370 K. The plots are labelled with the phases adopted by the material at each temperature. The powder patterns for  $2^{\text{C}}$  are noisier because they were obtained from nujol mull samples *in vacuo*.

As for **1**, the anhydrous phases of **2** produced by slow crystallisation ( $2^{\text{A}}$ ) and thermal dehydration of the dihydrate ( $2^{\text{B}}$ ) are distinct from each other by X-ray powder diffraction.

The variable temperature spin-state properties of phases  $2^{\text{B}}$  and  $1^{\text{B}}$  are again different. While  $1^{\text{B}}$  exhibits a highly cooperative spin transition centred near 205 K,<sup>7</sup>  $2^{\text{B}}$  remains high-spin upon cooling to 2 K (Fig. 3). In the powder diffractometer, cooling  $2^{\text{B}}$  below 295 K caused a transformation to a new phase  $2^{\text{C}}$ , which has a very different powder diffraction pattern (Fig. 2). The corresponding material  $1^{\text{B}}$  also converts to  $1^{\text{C}}$  under these conditions, at the slightly higher temperature of 303 K.<sup>7</sup> Phases  $2^{\text{B}}$  and  $2^{\text{C}}$  are isostructural with  $1^{\text{B}}$  and  $1^{\text{C}}$  (ESI†). However, whereas  $1^{\text{C}}$  transforms further to  $1^{\text{D}}$  on additional cooling, the phase  $2^{\text{C}}$  is retained between 120–250 K (Fig. 2 and 3). Hence,  $2^{\text{C}}$  (and presumably  $1^{\text{C}}$ ) are high-spin structures, and spin-crossover in **1** can only occur owing to the extra  $1^{\text{C}} \rightarrow 1^{\text{D}}$  phase change.

In addition to the above, single crystal X-ray analyses were obtained from two solvates of **2**. The methanol solvate  $2\cdot 2\text{CH}_3\text{OH}$

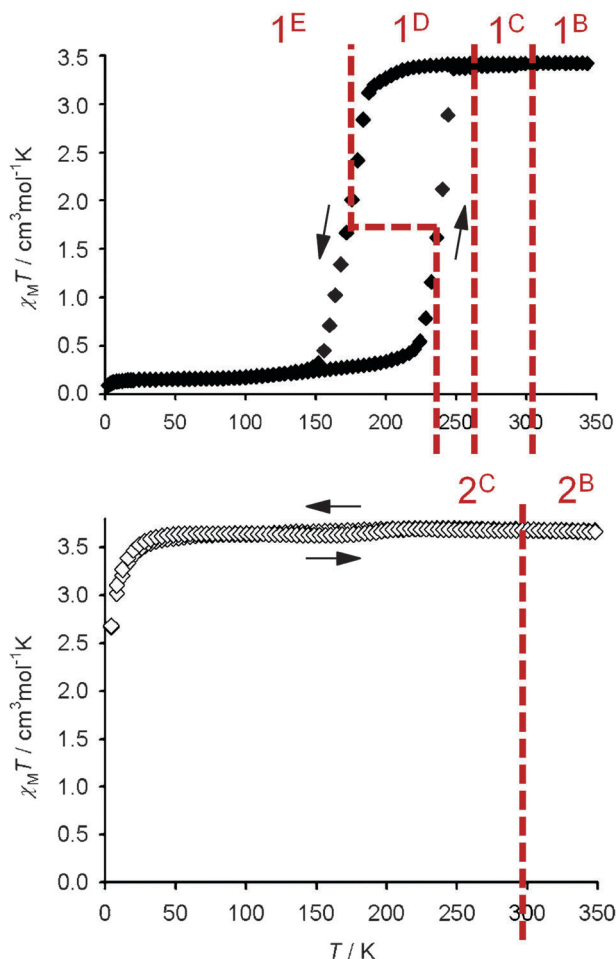


**Fig. 3** Comparison of the magnetic susceptibility behaviour of **1<sup>B</sup>** (◆, top)<sup>7</sup> and **2<sup>B</sup>** (◇, bottom), and their phase changes between 120 and 350 K. The red lines show the temperatures of each phase transition.

contains one formula unit per asymmetric unit, whose complex cation is low-spin at 150 K. The other solvate  $2 \cdot x\text{CH}_3\text{NO}_2 \cdot \frac{4}{3}(\text{C}_2\text{H}_5)_2\text{O}$  ( $x \approx 0.83$ ) contains three unique molecules in its asymmetric unit, one of which is low-spin at 150 K while the other two have a mixed high/low-spin population. Both structures contain extensive hydrogen bonding between the complex, anions and solvent (ESI†).

The complex cations in  $2 \cdot 2\text{H}_2\text{O}$ , **2<sup>A</sup>**, the corresponding phases of **1** and the solvate structures of **2** all associate into four-fold “terpyridine embrace” layers, through interdigitation of the pyrazolyl arms of neighbouring molecules.<sup>9,10</sup> These cation layers are separated in the lattice by sheets of anions and, where present, solvent. The cation layers in **2<sup>A</sup>** and  $2 \cdot 2\text{H}_2\text{O}$  are homochiral and contain strictly or approximately co-aligned complex molecules, with adjacent layers being related by a crystallographic inversion centre. In contrast, the layers in the solvate crystals contain molecules of both handedness, which are canted with respect to each other. The interplanar distance between adjacent, overlapping pyrazole rings in the layers varies from 3.3–3.9 Å in the four materials. Despite their individual differences, **1** and **2** clearly show a strong preference for this layered structure type, which allows some flexibility in

the orientation of the molecules. Hence, we suggest that the multiple phase changes in **1**, **2** and their hydrate materials might reflect facile, reversible canting of the cations in the terpyridine embrace layers, coupled to movement or (dis)ordering of the anions in the space between those layers. Such rearrangements could also lead to changes to the hydrogen bonding at the  $[\text{FeL}_2]^{2+}$  cations, which would further influence their spin states in the different phases.<sup>11</sup>

In conclusion, the complicated structural and spin-state chemistry of the  $[\text{FeL}_2]^{2+}$  system is even more complex than first reported.<sup>7</sup> The  $\text{BF}_4^-$  and  $\text{ClO}_4^-$  salts form dihydrate and anhydrous phases which are isostructural, but show contrasting spin-state behaviour. Thus,  $2 \cdot 2\text{H}_2\text{O}$  exhibits thermal spin-crossover but  $1 \cdot 2\text{H}_2\text{O}$  does not. Conversely, anhydrous **2<sup>B</sup>** is not spin-crossover active, while **1<sup>B</sup>** exhibits a highly cooperative spin-transition below room temperature. X-ray powder diffraction has demonstrated that these results reflect different sequences of phase transitions in the two sets of materials. Calorimetry and Mössbauer spectroscopic studies are in progress to shed more light on this unprecedented structural chemistry.

The authors thank Dr Tamsin Malkin (University of Leeds) for help with the powder diffraction data. This work was funded by the EPSRC, the University of Manchester and the University of Leeds.

## Notes and references

¶ X-ray diffraction data were collected from the same single crystal of  $2 \cdot 2\text{H}_2\text{O}$  at 296, 200 and 105 K. At 296 K the data were solved in  $I4_1/a$ , the space group adopted by  $1 \cdot 2\text{H}_2\text{O}$ , but refined poorly (crystals of  $1 \cdot 2\text{H}_2\text{O}$  produced by hydration of preformed **1<sup>A</sup>** show similar behaviour<sup>7</sup>). At the lower temperatures good quality refinements were achieved, but it was not possible to unambiguously assign a space group to the material. Despite these ambiguities, these crystallographic refinements confirm that the disposition of the molecules in  $2 \cdot 2\text{H}_2\text{O}$  is identical to that in  $1 \cdot 2\text{H}_2\text{O}$ .<sup>7</sup> They are also consistent with the magnetic susceptibility data in showing that  $2 \cdot 2\text{H}_2\text{O}$  has an approximate 1:1 high:low-spin population at 200 K, and is fully low-spin at 105 K. More details are given in the ESI.†

- 1 *Spin Crossover in Transition Metal Compounds I–III*, Top. Curr. Chem., ed. P. Gülich and H. A. Goodwin, 2004, vol. 233–235.
- 2 *Spin-crossover materials – properties and applications*, ed. M. A. Halcrow, John Wiley & Sons, Chichester, UK, 2013, p. 568.
- 3 A. Bousseksou, G. Molnár, L. Salmon and W. Nicolazzi, *Chem. Soc. Rev.*, 2011, **40**, 3313.
- 4 For recent reviews see: M. A. Halcrow, *Coord. Chem. Rev.*, 2009, **253**, 2493; P. Gamez, J. S. Costa, M. Quesada and G. Aromí, *Dalton Trans.*, 2009, 7845; J. Tao, R.-J. Wei, R.-B. Huang and L.-S. Zheng, *Chem. Soc. Rev.*, 2012, **41**, 703; P. Gülich, *Eur. J. Inorg. Chem.*, 2013, 581.
- 5 I. Šalitroš, N. T. Madhu, R. Boča, J. Pavlik and M. Ruben, *Monatsh. Chem.*, 2009, **140**, 695.
- 6 M. A. Halcrow, *Chem. Soc. Rev.*, 2011, **40**, 4119.
- 7 T. D. Roberts, F. Tuna, T. L. Malkin, C. A. Kilner and M. A. Halcrow, *Chem. Sci.*, 2012, **3**, 349.
- 8 Other examples of strongly hysteretic spin-crossover, whose structural chemistry is well understood, include: J.-F. Létard, P. Guionneau, E. Codjovi, O. Lavastre, G. Bravic, D. Chasseau and O. Kahn, *J. Am. Chem. Soc.*, 1997, **119**, 10861; M. Nihei, H. Tahira, N. Takahashi, Y. Otake, Y. Yamamura, K. Saito and H. Oshio, *J. Am. Chem. Soc.*, 2010, **132**, 3553; G. A. Craig, J. S. Costa, O. Roubeau, S. J. Teat and G. Aromí, *Chem.–Eur. J.*, 2011, **17**, 3120; H. J. Shepherd, T. Palamarcui, P. Rosa, P. Guionneau, G. Molnár, J.-F. Létard and A. Bousseksou, *Angew. Chem., Int. Ed.*, 2012, **51**, 3910.
- 9 I. Dance and M. Scudder, *CrystEngComm*, 2009, **11**, 2233.
- 10 R. Pritchard, C. A. Kilner and M. A. Halcrow, *Chem. Commun.*, 2007, 577.
- 11 S. A. Barrett, C. A. Kilner and M. A. Halcrow, *Dalton Trans.*, 2011, **40**, 12021 and refs. therein.